Int. J. Electrochem. Sci., 14 **(2019)** 9596 – 9609, doi: 10.20964/2019.10.45

International Journal of ELECTROCHEMICAL SCIENCE
www.electrochemsci.org

Corrosion behavior of multilayer coatings deposited by PVD on Inconel 718 in Chloride and Sulphuric Acid solutions

F. Almeraya-Calderón[1]., M. Montoya-R[1], N. Garza Montes de Oca[1]., J.H. Castorena G[2]., F. Estupiñan L[1]., J.Cabral M[1]., E. Maldonado B[3]., C. Gaona-Tiburcio[1].*
[1]Universidad Autónoma de Nuevo León. FIME – CIIIA. Av. Universidad s/n. Ciudad Universitaria. San Nicolás de los Garza, Nuevo León, México.
[2]Universidad de Autónoma de Sinaloa. Facultad de Ingeniería Mochis, Los Mochis, Sinaloa, México
[3]Universidad Veracruzana. Facultad de Ingeniería Civil. Xalapa, Veracruz. México

[*]E-mail: falmeraya.uanl.ciiia@gmail.com

Received: 10 July 2019 / *Accepted:* 9 August 2019 / *Published:* 30 August 2019

The corrosion behavior of multilayer AlCrN/TiSi, AlCrN/TiCrSiN and AlCrN/AlCr + Cr coatings deposited by physical vapor deposition (PVD) technique was investigated Electrochemical techniques such as linear polarization resistance (RPL) and potentiodynamic polarization (PP) were used to study the corrosion behavior performance of the multilayers PVD coatingsAfter electrochemical testing, the coating surface morphology was analysed by scanning electron microscopy (SEM) and the atomic composition by energy dispersive X-ray spectroscopy (EDS). The results of the corrosion potential indicated that there was no pattern of the behavior corrosive of the coatings in NaCl and H_2SO_4 test solutions. The corrosion rates of the different systems are in the range between 1E-3 mm/year and 1E-2 mm/year in NaCl and H_2SO_4 test solutions, respectively. Some coatings showed tendency to the pseudo passivation behavior in the different electrolytes with a positive hysteresis, which indicative of localized corrosion. For H_2SO_4 the most stable coating was for AlCrN/TiSi. PVD coatings present the highest corrosion rate in H_2SO_4, and both AlCrN/TiSi and AlCrN/AlCr + Cr present corrosion localized. AlCrN/AlCrN+CrN coating has lower pitting corrosion resistance

Keywords: Corrosion, PVD, Inconel 718, multi-layer coatings.

1. INTRODUCTION

The change of the physical properties of the surfaces of materials can be obtained by a wide variety of coating types and coating deposition technologies, even with processes that do not require material deposit 1. During the lasts years the Physical Vapor Deposition (PVD) technique has been used as a technique for depositing protective layers with good surface properties such as corrosion resistance, good wear resistance, high hardness and friction with excellent adhesion to the substrate 2.

Multi-component coatings such as TiAlN, TiSiBN, TiCrN and AlCrN have been sintered by PVD with good surface and mechanical properties 3, nevertheless the multilayers transitional nitrides/nitrides coating have been subjected to great interest due which possess a high hardness as well as a high toughness than homogenous coatings 4, also provides oxidation and corrosion resistance 5. Multi-layer systems such as Ti /CrN and Ti/ TiAlN coatings deposited by PVD were studied depending on the number of layers on brass, it was shown that the number of layers resulted in improved corrosion resistance, thus the formation of multilayer structure can be an alternative in improving the oxidation resistance 6. TiAlN/CrN coatings was deposited to combine the high hardness and good oxidation resistance of TiAlN and the good thermal stability of CrN. In addition, a monolayer TiAlSiN and multilayer TiAlSiN/CrAlN coating was deposited by cathodic arc ion-plating method and oxidation resistance was studied at high temperature. The two combinations yielded a coating with good wear resistance and oxidation resistance, however, the multilayer TiAlSiN/CrAlN coating showed superior oxidation resistance compared to monolayer TiAlSiN coating. Likewise, it was reported that the additional amount of Al content of CrAlN to the TiAlSiN system prompt a formation of solid oxide layer of Al and Si-rich oxide on the top surface by forming a multilayer structure 7.

Another multi-layer report concluded that at least one $(Al_yCr_{1-y})X$ layer $(0.2 \leqq y \leqq 0.7)$, wherein X is one of the following elements N, C, B, CN, BN, CBN, NO, CO, BO, CNO, BNO, CBNO, but preferably N or CN, and/or a (Ti_zSi_{1-z}) layer $(0.99 \geqq z \geqq 0.7)$ improve wear resistance 8. Currently there are no reports of multilayer systems with less than one layer of AlCrN on Inconel 718 where corrosion kinetics is evaluated. The aim of this work was to study the corrosion behavior of multilayered coatings (AlCrN/TiSiN, AlCrN/TiCrSiN and AlCrN/AlCrN+CrN) deposited by PVD on Inconel 718 in Chloride and Sulphuric Acid test solutions.

2. EXPERIMENTAL

2.1. Substrate material.

Nickel-base alloy 718 were used as substrate material (Table 1). Before coating deposition all substrates were ultrasonically cleaned in an alkaline solution heated to 333 K and thereafter in ethanol for 5 min each and then dried in nitrogen air.

Table 1. Chemical composition of Nickel-base alloy 718 (wt.%)

Material	Ni	Fe	Cr	Mo	Nb	Ti	C	Si
Alloys 718	51.7	20.2	18.18	3	5.22	0.96	0.02	0.1

2.2. Coating deposition.

The coatings were deposited in a commercial Blazer's Oerlikon machine. For all coatings, a pure reactive N_2 (99.99%) atmosphere was used during deposition. The eight sources of machine (Al 70% Cr

30% of the customized sintered targets by atoms) were used to deposit the AlCrN coating as bottom layer at 450 °C. The temperature of the top layers during deposition was held at approximately at 350 °C for the TiSiN and TiN+CrSiN coatings layers and 450 °C for the AlCrN+CrN coating layer. The summary of the process parameters is presented in Table 2. The coatings are identified as in Table 3.

Table 2. Summary of the coating deposition parameters.

Parameters	*Values with units*
Argon flow rate	800 sccm
N2 flow rate	1100 sccm
Chamber pressure	3.2 E-4 mbar
Current/voltage	50/200 V

Table 3. Sample classification.

Samples	*Coating*
SR	Alloys Inconel 718
R1	AlCrN/TiCrSiN
R2	AlCrN/AlCrN+CrN
R3	AlCrN/AlCrN+CrN

2.3. Microstructural characterization.

The surface morphology in cross-section of the coated samples and substrate. was used to observe with Scanning electron microscope (SEM) and energy dispersive X-ray spectroscopy (EDS). Micrographs were taken at 2000X. The equipment used was a SEM Jeol JSM 6510LV series.

2.4. Electrochemical tests.

A conventional 3-electrode cell configuration was used for electrochemical studies. The multilayered coatings deposited by PVD on Inconel 718 were used as the working electrode. A saturated calomel electrode (SCE) and a platinum mesh were used as reference and counter electrode, respectively. Electrochemical measurements were carried out using a Gill-AC potentiostat/galvanostat/ZRA from ACM Instruments. The Linear Polarization Resistance (LPR) were recorded at a sweep rate of 10 mV/min at, A potential scan range was applied between -20 to +20 mV vs. ESC., according to ASTM G59 standard [9]. Potentiodynamic polarization curves were recorded at a sweep rate of 60 mV/min, A potential scan range was applied between −300 mV and +1500 mV vs. SCE., according to ASTM G61 standard [10].

Corrosion experiments were performed by immersion of the coated samples, with an exposed surface area of 1.0 cm^2, in a 5% NaCl and 1% H_2SO_4 solution, at 25 ºC temperature.

3. RESULTS AND DISCUSSION

3.1. Microstructural Analysis.

The SEM Micrograph and EDS spectra are shown in Figures (1-4). The elemental composition of Inconel 718 (SR) substrate are shown in Fig 1, which shows that presence of Ni, Cr, Fe and other elements were detected indicating a correspondence of the elements with alloys 718 11.

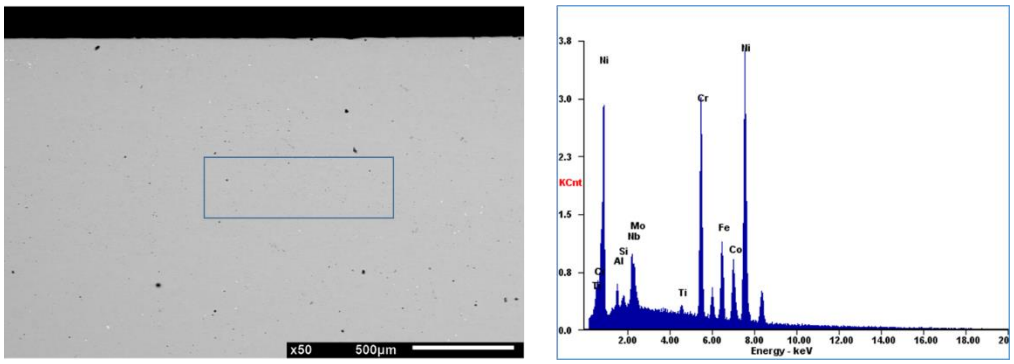

Figure 1. SEM cross-section micrograph and EDS of SR (Alloys Inconel 718).

Figure 2 shows the cross-sectional view of the coating AlCrN/TiSiN (R1), which reveals that the TiAlN (top) and AlCrN (bottom) layers of the coating over the substrate. Both the substrate and the aluminum, chromium and nitrogen elements of the first layer (blue region) are shown distributed homogeneously bonding on the substrate with a well-defined bottom layer/substrate interface. Likewise, the top layer was identified with elements such as titanium, silicon and nitrogen, which according to the semiquantitative calculations from EDS analysis the concentration is 39, 6 and 22 wt %, respectively; however, did not present a homogeneous and compact bonding with the bottom layer due to interdeffusion in which the atoms of the top layer did not diffuse into the bottom layer 12.

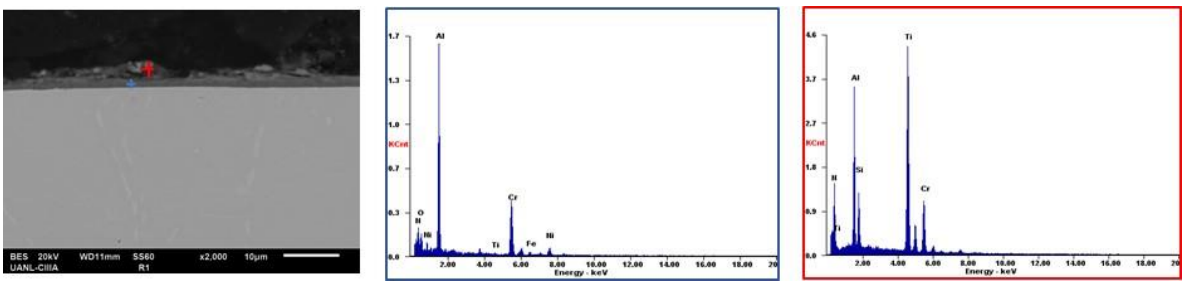

Figure 2. SEM cross-section micrograph and EDS of R1 coating (AlCrN/TiCrSiN).

The SEM cross-section micrograph and elements analysis in the EDS spectra of AlCrN/TiCrSiN (R2) coating in Fig.3 shows elements such as Ti, Cr, Si, N, Co and Al. Also, there are energy dispersion for iron and nickel corresponding to the base material (Inconel 718). It is clear a greater energy dispersion of Al and Cr, which can be associated to the AlCrN/CrTiSiN multilayer, but the different interfaces cannot be identified by SEB cross-section.

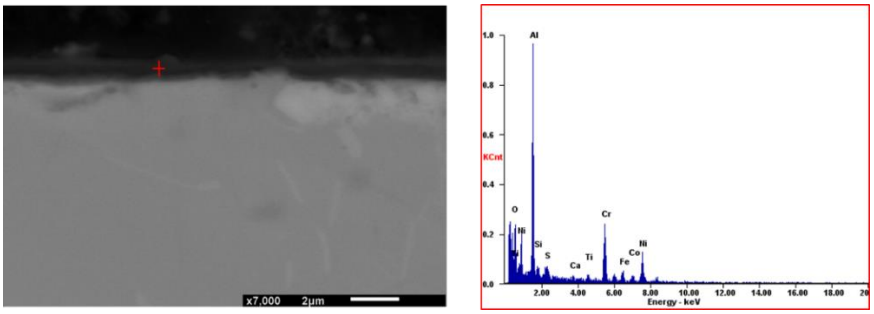

Figure 3. SEM cross-section micrograph and EDS of R2 coating (AlCrN/CrTiSiN).

On the other hand, as reveal the SEM images of PVD AlCrN/AlCrN+CrN (R3) coating in Fig. 4 a compact morphology and it was possible to identify two phases in R3. The darker contrast of the layers is associated with AlCrN due to its high content of aluminum as opposed to the top layer. This type of AlCrN/AlCrN + Cr coating allowed a clear determination of the structure [13-14]. It should be noted that due to the proportionality of Cr content in layer b (AlCrN + Cr) compared with layer AlCrN there is a greater dispersion energy in the surface layer (red EDS).

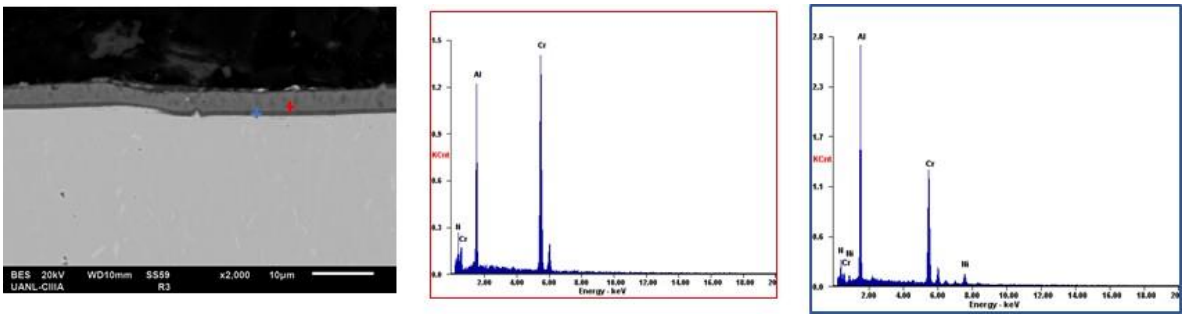

Figure 4. SEM cross-section micrograph and EDS of R3 coating (AlCrN/AlCrN+CrN).

3.2. Corrosion behavior of PVD coating and substrate.

The corrosion behavior of the substrate and coatings was studied by Linear Polarization Resistance (LPR) and cyclic polarization potenciodynamic curves. From the LPR the polarization resistance value was obtained in the range of ± 20 mV vs ESC. The current density and corrosion potential were obtained by extrapolating the Tafel curves for each system in each of the test solutions.

The significant corrosion parameters are listed in Table 4 and Table 5 including LPR, corrosion potential E_{corr}, corrosion current density i_{corr} and corrosion rate *C.R* measured.

Table 4 Error! No text of specified style in document.**.** Electrochemical parameters of R1, R2 and R3 coatings deposited in alloys Inconel 718 (SR) in a 5 wt % NaCl solution.

System	LPR [Ω/cm2]	E_{corr} [mV/SCE]	i_{corr} [mA/cm^2]	C.R [mm/yr]
SR	89.356	374	0.00206	0.02162
R1	28463	-58	0.00137	0.01546
R2	38794	-74	0.00033	0.00380
R3	1312.9	-58	0.00040	0.00450

Table 5. Electrochemical parameters of R1, R2 and R3 coatings deposited in alloys Inconel 718 (SR) in a 1 wt % H_2SO_4 solution.

System	LPR [Ω/cm^2]	E_{corr} [mV/SCE]	i_{corr} [mA/cm^2]	C.R [mm/yr]
SR	29.42	426	0.00145	0.01525
R1	76.62	217	0.00075	0.00844
R2	40.489	353	0.00557	0.06257
R3	66.585	-10	0.00646	0.07257

The behavior of E_{corr} in the PVD coating indicated that there was no pattern of the behavior corrosive of the coatings, however, only in the substrate presented a noble potential for the different solutions. On the other hand, can be seen that for R3 coating has a meaningfully higher corrosion potential (41 mV/SCE) in different solutions and lower anodic current density than other coatings in H_2O solution. These results indicate that the R3 coatings exhibit better electrochemical performance than the uncoated, R1 and R2 coatings due to more noble corrosion potential. The corrosion behavior of R1 coating submerged in NaCl solution presented a more noble potential (-58 mV/SCE) than those reported in 15, in which monolayers of TiSiN coating presented an E_{corr} between -261 and -118 mV/SCE which could be related to the fact that a multilayer coating is more corrosion resistant than a monolayer coating in this electrolyte. In the electrochemical behavior of TiN/TiAlN multilayers 16 study was indicated that TiN/TiAlN multilayer coating had superior corrosion resistance in 3.5% NaCl solution compared with monolayer of TiN and TiAlN coatings. Besides, it was reported that E_{corr} was found much lower in TiAlN than that TiN layer with the addition of Al into TiN coating to form the ternary coating. A positive shift of E_{corr} from -635 to -377 mV/SCE was presented for TiSiN with the addition of Al element to form TiAlSiN coating. According to more active lower potential, the TiAlSiN coating with high corrosion potential represented its excellent corrosion resistance, these results can be attributed to the formation of

the passivation Al-oxidation reaction products when the TiAlSiN film was immersed in corrosive medium 17.

On the other hand, the large amount Cr element in AlCrN/AlCrN+Cr (R3) can be related with the enhances the resistance corrosion in test solutions due the presence of a passive layer leads 18, which provide an additional resistance to the corrosive medium passing through the pores as long interfaces increases - more numbers of micro-pores are blocked. Otherwise, when R3 coating was submerged in H_2SO_4 solution in which E_{corr} is most negative suggesting that the smallest driving force was required to initiate the corrosion in H_2SO_4 solution.

A study of the corrosion behavior in H_2SO_4 solution of TiSiN/TiAlN nanoscale multilayered coatings reported a better corrosion resistance for the multilayered TiSiN/TiAlN coatings (-10 to 80 V/SCE) than the TiAlN coating 19, noble values as reported for the corrosion potential for AlCrN/TiSiN (R1) in this investigation in H_2SO_4 solution (-740 mV/SCE).

The LPR parameter is correlated with the corrosion rate. It has been proven that the lower corrosion rates can be obtained in the higher polarization resistance 20. In the H_2SO_4 solution the LPR varied between 29 to 66 Ω/cm^2. In NaCl solution the substrate and PVD coatings showed intermediate values of LPR with respect to the other solutions, which can be related as a solution less aggressive than H_2SO_4.

Then again, the effect of adding Al and Si elements plays a major role on corrosion resistance in Ti-based coatings in 3.5 wt.% NaCl aqueous sodium chloride solutions 16. In which investigation was reported corrosion currents density of 0.56 and 0.16 $\mu A/cm^2$ that would correspond to the corrosion rate of 6E-3 and 1E-3 mm/year for TiN and TiAlSiN respectively. The behavior corrosion of multilayer CrAlN/SiN coatings was studied in 21. Corrosion current density between 0.005 to 0.045 $\mu A/cm^2$ corresponding to rate corrosion of 8E-3 and 5E-4 mm/year were found in 3.5 wt % NaCl solution at room temperature. In the case of multilayer PVD coatings presented in this investigation a lower corrosion rate for AlCrN/TiCrSiN (R2) and AlCrN/AlCrN +CrN (R3) coatings in which have a corrosion rate of 3.8E-3 mm/year and 4.5E-3 mm/year, respectively, values close to those reported for TiN coating and basically for TiAlSiN, and multilayer CrAlN/SiN. The rate corrosion for AlCrN/TiSiN (R1) coating in NaCl solution were in the range 1E-2 mm/year. Consequently, the addition of Cr in at least one layer of the multilayer improved the corrosion rate in multilayer PVD in NaCl solution. In the case of the samples exposed in H_2SO_4 the corrosion rates presented an inverse behavior as in NaCl solution; the corrosion rate of R2 and R3 coating is found lower than SR and R1 coatings.

Cyclic Polarization potenciodynamic curves measurements were performed in order to determine corrosion behavior when placed in the different electrolyte solutions. The Figure 5 and 6 present cyclic polarization measurements for the PVDs coatings including the Inconel 718 substrate obtained in test solutions.

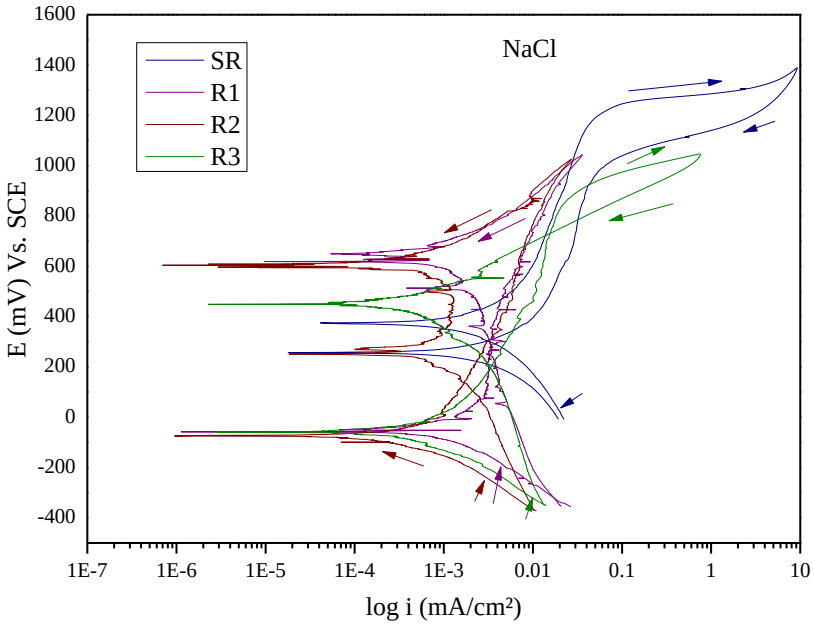

Figure 5. Cyclic Potentiodynamic polarization curves of PVD coating including substrate immersed in 3.5% NaCl solution.

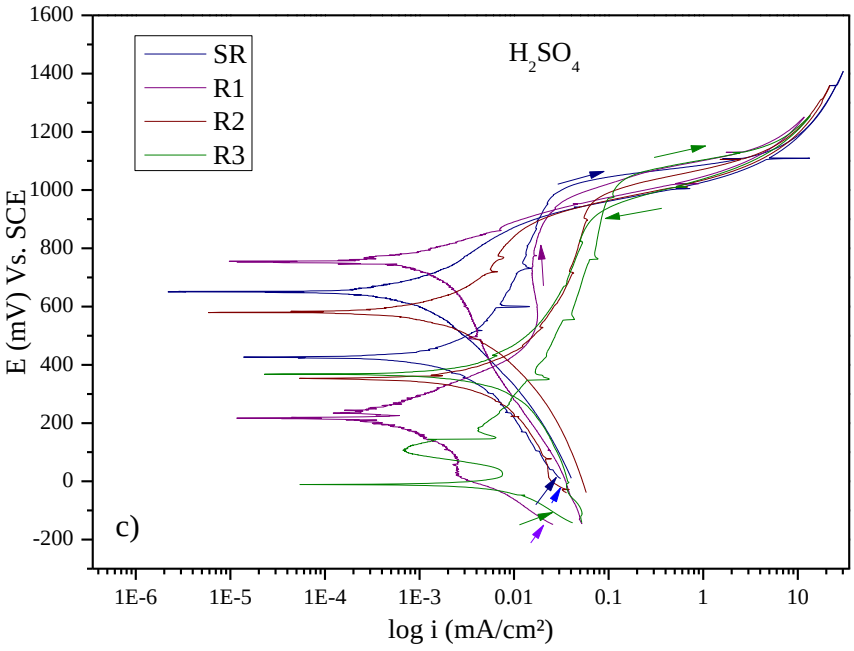

Figure 6. Cyclic Potentiodynamic polarization curves of PVD coating including substrate immersed in 1% H_2SO_4 solution.

A mixed activation in the anodic and cathodic branches in all systems was presented. From the corrosion potential a linear relationship in current density is present for all systems, this increasing can be related to a corrosion phenomenon (“active region"). All systems in NaCl and H_2SO_4 solutions of both Inconel 718 substrate and R1, R2 and R3 coatings indicate pseudopasivation regions, This indicates that the metal dissolution behavior of the alloys in this environment is active corrosion. This might be ascribed to the presence of a high H^+ concentration, leading like result a strong general corrosion possible 22.

The critical potential above which the corrosion current increases abruptly with increasing applied potential can be defined as “pitting potential, E_{pit}”. An increase of E_{pit} to a more positive value can be taken as an indication that the coating/substrate system is getting more localized corrosion resistant. It is important to mention that a pitting is localized corrosion attack in which small pits or holes form. They ordinarily penetrate from the top of a horizontal surface downward in a nearly vertical direction 23.

Table 6. Pitting potential of PVD coating in test solution.

Systems	Pitting potential E_{pit}	
	NaCl [mV/SCE]	H_2SO_4 [mV/SCE]
SR	1195	975
R1	-	943
R2	-	920
R3	835	1016

Table 6 presents the pitting potential of Inconel 718 substrate (SR) and PVDs coatings (R1, R2 and R3). On the one hand, both R1 and R2 in NaCl solution, respectively, did not present pitting potential, it could indicate high resistance to localized corrosion 24. The physical origins behind the negative hysteresis can be related with the passive film thickness on potential and subsequent dissolution rate, therefore, passive films grow thicker at higher potentials and after longer times at a constant potential.

On the other hand, the E_{pit} of Inconel 718 is more positive than AlCrN/AlCrN +CrN (R3) coating E_{pit}, which indicates that Inconel 718 has better resistance to pitting corrosion in the NaCl solution in which only SR and R3 presents pitting potential. An active, passive, and transpassive regions show that alloy 718 exhibits passive behavior in 3.5 wt.% NaCl 25. Was observed that E_{pit} for this superalloy 718 was 1.05 $V_{(Ag/AgCl/Sat.\ KCl)}$ at room temperature, however, this electrochemical value decreases in function of temperature [25]. The E_{pit} was around 1200 mV/SCE for NaCl solution. The anodic current for H_2SO_4 solution continues to rise as increasing potential applicated allowing a smaller E_{pit}. The active values for observed in H_2SO_4 solution can be attributable to the enhanced activity of hydrogen ions in the acid media 25.

However, in H_2SO_4 solution all systems presented pitting corrosion in which R3 coating had better resistance to pitting corrosion (1016 mV/SCE). Once the potential is raised above E_{pit}, the systems entered the transpassive range and undergoes pitting corrosion leading to the initiation and propagation of pitting. As expected, numerous pits appear on the surface of systems, suggesting that a pitting mechanism takes place and the dissolution of the corrosion products can be appear [21, 26].

For systems that had pitting potential (table 6) the current rise continues even after scan reversal (breakdown potential). A positive hysteresis loop, which physical origins behind the stability of localized corrosion sites and the competition between diffusion and dissolution at localized corrosion sites was obtained for some systems. Hysteresis loop allows the pitting protection potentials (E_{pp}) to be determined (Table 7). The E_{pp} is defined as the point where the reverse scan intersects the forward scan and corresponds to the potential values below which pitting not occurs and above which pit nucleation begins [24-27]. A high value of E_{pp} may indicate a lower susceptibility for localized corrosion to occur as the case of R3 coating in all electrolytes, however, this electrochemical parameter depends of pitting corrosion potential. For this reason, an absolute measure of corrosion resistance can be defined as the difference between the E_{pit} and the E_{pp}, i.e., $DE = E_{pit}-E_{pp}$. The magnitude of DE is an indicator of pitting resistance, that is, the higher the DE value a lower the pitting resistance 28.

Table 7. Pitting protection potentials of PVD coating in test solution.

Systems	Pitting protection potential, E_{pp}	
	NaCl [mV/SCE]	H_2SO_4 [mV/SCE]
SR	307	903
R1	-	920
R2	-	950
R3	720	929

Table 8. Indicator of pitting resistance of PVD coating in test solution.

Systems	$DE = E_{pit}-E_{pp}$	
	NaCl [mV/SCE]	H_2SO_4 [mV/SCE]
SR	888	72
R1	-	23
R2	-	36
R3	115	87

The result based on table 8, indicates that the AlCrN/AlCrN +CrN (R3) coating had lower pitting corrosion resistance in H_2O solution due the area under the curve of positive hysteresis can be greater than in NaCl solution. In case of systems preformed in H_2SO_4 solution a quick repassivation occurred. This may suggest high susceptibility to local thinning and dissolution for the oxide layer in NaCl solution for Inconel 718. An inverse behavior for R3 coating was presented [29-30].

In H_2SO_4 solution both Substrate and coatings presented susceptibility to localized corrosion, nevertheless, DE values are smaller than other electrolytes which can be related to the passivity of surface. The elements such as Cr, Ti, Al and Si can allow highest electrochemical activity in this corrosive electrolyte. As a result, a protective chromium oxide film is preferentially created on the surface, which facilitates the improvement of the corrosion resistance 31. In this reference was reported pitting corrosion around 900 mV/SCE for AlTiN, AlCrN and AlCrSiWN coatings in a 3.5 wt% NaCl solution, values according to R3 in this solution, however, they not done a complete cycle in performance electrochemical technique, for this reason no was possible evaluate E_{pp}.

The existence of the passive region in PVD nitrures coatings is due to the formation of a thin oxide passive layer on surface 32 when the coating is contacting the NaCl solution or other aggressive solution, which seals pores in the coating inhibiting electrolyte diffusion to the substrate surface 33. In this reference, the corrosion behavior of the CrAlN and TiAlN coatings in a NaCl solution was performed. It was showed as the potential (mV/SCE) becomes more positive, the corrosion reaches the substrate though the pinholes. A film can be generated but due to the immerse time or the applied potential increased the film broke down finally. As a result, the pitting corrosion becomes the main corrosion mechanism in both hard coatings as follows it is presented: pitting corrosion of 370 and 740 mV/SCE, respectively, for CrAlN and TiAlN coatings. In 34 the corrosion behavior for multilayer Cr/CrN coating was performed. Pitting corrosion around 1000 mV/SCE was reported, it was due to rupture of the passive layer. This value for pitting corrosion was closer to those obtained in our investigation.

The metal substrates under PVD coatings could show a corrosion attack 35 due that these hard coatings present inherent defects such as pinholes, microcracks and macroparticles that are generated during the deposition process. These defects can allow the existence of preferential diffusion paths of aggressive solutions such NaCl and H_2SO_4 into the substrate through the protective coating film causing localized corrosion too 36. This would be the reason why AlCrN/TiCrSiN (R2) and AlCrN/AlCrN +CrN (R3) coating had more corrosion resistance than SR and R1 coatings as reported in 37 which the anodic current density value of CrSiN is lower than that of CrN, this behavior can be attributed to the denser structure and less cracks and pinholes of the coating.

A Study 13 of corrosion behavior of monolayer TiN and TiAlN/TiAlCrN multilayer demostred a passive behavior in HCl solution. In the case of TiAlN/TiAlCrN coated condition undergoes localized corrosion at 0.83 mV/SCE. It is worth mentioning that AlCrN/AlCrN +CrN (R3) coating presented in its microstructure of morphology many interfaces and a homogeneous microstructure, which lead to improved corrosion resistance. Also, a higher concentration of Cr improves the corrosion resistance due to the formation of a passive Cr_2O_3 plus a possible Al_2O_3 layer on the surface of the coating 38, for this reason, is possibly related a passive behavior in H_2SO_4 solution 39 and a tendency to passivation in the other solutions, including the other coating systems R1 and R2 coatings which presented a similar trend.

In order to evaluate the protective efficiency (P %) of coating it was calculated from the potentiodynamic polarization values (table 3,4 and 5) [40-42].

$$P(\%) = \left(1 - \frac{i_{corr}}{i_{corr}^{0}}\right) * 100$$

Where i_{corr} and i_{corr}^{0} denoted the corrosion current densities of the coating and substrate, respectively. The calculated protective efficiencies are presented in Table 9.

Table 9. Protective efficiency of PVD coating in test solution.

System	Protective efficiency [%]	
	NaCl	H_2SO_4
R1	33.4	48.4
R2	83.6	---
R3	80.6	---

All systems in NaCl were positive protective efficiency R1 (33.4%), R2 (83.6%) y R3 (80.6%) The R2 and R3 PVD Coating in H_2SO_4 test solution does not protect the Inconel 718 substrate. The lower corrosion resistance of the in theses coatings can be related mainly determined by its microstructure that provides pinholes running quasi perpendicular to the coating/substrate interface that are considered rapid paths for corrosive medium to pass through [40-41].

4. CONCLUSIONS

- A study of corrosion behavior of multilayer PVD coatings in NaCl and H_2SO_4 solutions was presented. The AlCrN/TiSiN (R1) and AlCrN/TiCrSiN (R2) coatings did not present a homogeneous and compact bonding with the bottom layer and substrate, it could have been due to lack interdeffusion in which the atoms of the top layer did not diffuse into the bottom layer and substrate, respectively.
- The most electrochemically active solution was acidic H_2SO_4 solution in which the corrosion rates were in the range 1E-2 mm/year.
- The corrosion mechanism presented for the different systems exposed in NaCl solution was related in the following way: SR coating: localized corrosion, R1 and R2 coatings: generalized corrosion and R3 coating: localized corrosion.
- The systems in H_2SO_4 solution presented tendency to psudo-passivation in most coatings. Both for SR substrate, R1 and R3 coatings could be related to a susceptibility to localized corrosion and R2 coating had a negative hysteresis loop which can be linked to a high resistance to localized corrosion in H_2SO_4 solution. From DE analysis indicates that the AlCrN/AlCrN+CrN (R3) coating has lower

pitting corrosion resistance, this may suggest that larger driving force is required to repassivation pitting corrosion.

ACKNOWLEDGEMENTS
The authors would like to acknowledge the work group UANL-CA-316.

References

1. L.A. Dobrzanski, D. Pakula, M. Staszuk, Chemical Vapor Deposition in Manufacturing, (2013) Springer-Verlag. London, England.
2. L.A. Dobrzanski, D. Pakula, M. Staszuk, Handbook of Manufacturing Engineering and Technology, (2015) Springer-Verlag. London, England.
3. T. S. Kumar, S. B. Prabu, G. Manivasagam, *J. Mater. Eng. Perform.*, 23 (2014) 2877.
4. M. Nordin, M. Larsson, S. Hogmark. *Surf. Coat. Technol.*, 106 (1998) 234.
5. Ö. Baran, E. E. Sukuroglu, I. Efeoglu, Y. Totik, *J. Adhes. Sci. Technol.*, 30 (2016) 2188.
6. L. A. Dobrzański, K. Lukaszkowicz, A. Križ, *J. Mater. Process. Technol*., 143 (2003) 832.
7. N. Fukumoto, H. Ezura, T. Suzuki, S*urf. Coat. Technol*., 204 (2009) 902.
8. V. Derflinger, U.S. Patent and Trademark Office, Patent No. 7,718,043, (2010).
9. ASTM G59-09. Standard test method for conducting potentiodynamic polarization resistance measurements, (2009), West Conshohocken, PA. USA.
10. ASTM G 61-86. Standard test method for conducting cyclic potentiodynamic polarization measurements for localized corrosion susceptibility of iron- nickel- or cobalt-based alloys, (2009), West Conshohocken, PA. USA.
11. A. Mortezaie, M. Shamanian, *Int. J. Pres. Ves Pip.*, 116 (2014) 37.
12. T. S. Kumar, S. B. Prabu, G. Manivasagam*, J. Mater. Eng. Perform.*. 23 (2014) 2877.
13. V. M. C. A. Oliveira, C. Aguiar, A. M. Vazquez, A. Robin, M. J. R. Barboza, *Corros. Sci.*. 88 (2014) 317.
14. J. Calderón, Ó. Mattos, O. Barcia, *Rev. Fac. Ing-Univ. Ant*., 38 (2006) 20.
15. A. F. Movassagh, A. Z. Abdollah, M. Aliofkhazraei, M. Abedi, *Wear*, 390 (2017) 93.
16. R. Ananthakumar, B. Subramanian, A. Kobayashi, M. Jayachandran, *Ceram. Int.*, 38 (2012) 477.
17. C. L. Chang, J. W. Lee, M. D. Tseng, *Thin Solid Films*, 517 (2009)5231.
18. W.Y.H. Liew, J.L.L. Jie, L.Y. Yan, J. Dayou, C.S. Sipaut, M. Faizah Bin Madlan, *Procedia Eng*, 68 (2013) 512.
19. C. L. Chang, W. C. Chen, P. C. Tsai, W. Y. Ho, D. Y. Wang, *Surf. Coat. Technol.*, 202 (2007) 987.
20. F. Movassagh-Alanagh, A. Abdollah-zadeh, M. Aliofkhazraei, M. Abedi, *Wear*, 390 (2017) 93.
21. S.H. Tsai, J.G. Duh*, J. Electrochem. Soc.,* 157 (2010) K89.
22. P. Kritzer, *J. Supercrit. Fluids*, 29 (2004) 1.
23. X. Z. Ding, A. L. K. Tan, X. T. Zeng, C. Wang, T. Yue, C. Q. Sun, *Thin Solid Films*, 516 (2008) 5716.
24. L.M. Calle, R.D. Vinje, and L.G. MacDowell, "Electrochemical Evaluation of Stainless Steels in Acidified Sodium Chloride Solutions," CORROSION/2004, Paper No. 04303 (Houston, TX: NACE 2004).
25. T. Chen, J. Nutter, J. Hawk, X. Liu, *Corros. Sci.*, 89 (2014)146.
26. C.-K. Lin, W.-C. Fan and W.-J. Tsai, *Corrosion*, 58 (2002) 904.
27. M.A. Amin, Arab, *J. Chem.*, 6 (2013) 87.
28. Z. F. Yin, W. Z. Zhao, W. Y. Lai, X. H. Zhao, *Corros. Sci.*, 51 (2009) 1702.
29. G. S. Frankel, J. *Electrochem. Soc.*, 145 (1998) 2186.

30. P. Marcus, V. Maurice, H. H. Strehblow, *Corros. Sci.*, 50 (2008) 2689.
31. L. Zhang, Y. Chen, Y. Feng, S. Chen, Q. Wan, J. Zhu, *Int. J. Refract. Metals Hard. Mater.*, 53 (2015) 68.
32. C. Mendibide, P. Steyer, J.-P. Millet, *Surf. Coat. Technol*., 200 (2005) 109.
33. Xing-zhao Ding, A.L.K. Tan, X.T. Zeng, C. Wang, T. Yue, C.Q. Sun, *Thin Solid Films*, 516 (2008) 5716.
34. M. Fenker, M. Balzer, H. Kappl, *Thin Solid Films*, 515 (2006) 27.
35. C.-C. Lin, K.-L. Chang, H.C. Shih, *Appl. Surf. Sci.*, 253 (2007) 5011.
36. R. Antunes, A. Rodas, N. Lima, O. Higa, I. Costa, *Surf. Coat. Technol.*, 205 (2010) 2074.
37. L. Shan, Y.R. Zhang, Y.X. Wang, J.L. Li, X. Jiang, J.M. Chen, *Trans. Nonferrous Met. Soc. China*, 26 (2016)175.
38. H.C. Barshilia, B. Deepthi, K.S. Rajam, K.P. Bhatti, S. Chaudhary, *J. Vac. Sci. Technol.*, 27 (2009) 29.
39. L. Cunha, M. Andritschky, L. Rebouta, and K. Pischow, *Surf. Coat. Technol.*, 116–119 (1999) 1152.
40. A.A. Matei, I. Pencea, M. Branzei, D.E. Trancă, G. Ţepeş, C.E. Sfăt, E. Ciovica , A.I. Gherghilescu, G.A. Stanciu, *Appl. Surf. Sci., 358* (2015) 572.
41. D. Zhou, H. Peng, L. Zhu, H. Guo, S. Gong, *Surf. Coat. Technol.*, 258 (2014) 102.
42. M. Chen, W. Chen, F. Cai, S. Zhang, Q. Wang, *Surf. Coat. Technol.*, 296 (2016) 33.
43. E. Marin, L. Guzman, A. Lanzutti, L. Fedrizzi, M. Saikkonen, *Electrochem. Commun.,* 11 (2009) 2060.